High-power tests of expanded beam connectors for co-packaged optics applications

Martin Hempstead*[a], Riley S. Freeland[a], Stephen Q. Smith[a], Sean B. Treacy[a], Sharon Lutz[b], Sherri Dempsey[b], Arnold Deal[b], Thomas Mitcheltree[b], Michael Kadar-Kallen[b], Erman Timurdogan[c] and Albert Benzoni[d]

[a]Corning Research and Development Corp., 1 Science Center Drive, Painted Post, NY 14870; [b]US Conec, Hickory, NC 28602; [c]Lumentum, San Jose, CA 95131; [d]Los Angeles, CA 90210

ABSTRACT

Co-Packaged Optics is a development of technology for high speed data switching, to be implemented widely in data center and high-performance computing architectures as a means to continue expansion of bandwidth and reduction of energy per bit. This development removes transceivers from the switch faceplate and replaces them with an optical link from the faceplate to transceiver PICs packaged on or near the ASIC switch substrate. Most approaches involve CW external lasers being carried over polarization-maintaining fiber to the PICs to be modulated for outgoing traffic. Lasers are active components with extremely high power densities and thus a relatively high failure rate, and they perform poorly at high temperatures such as prevail near the switch package. Therefore they will be remotely located or in removeable/front-panel pluggable packages that can be replaced with minimal disruption; this will require the use of optical fiber connectors.

System reliability is significantly enhanced by using fewer, higher-power lasers, so very high powers are anticipated for these sources, up to and perhaps exceeding 250 mW, and any connector must be able to reliably tolerate these power levels over the lifetime of the laser or switch box. The use of expanded beam connectors reduces the optical intensity at exposed surfaces compared to PC connectors, and may mitigate some potential issues.

We report on our initial studies to address this question of connector performance at these extreme conditions, with results on expanded beam single-mode connectors carrying high laser power in the O-band over many hundreds of hours.

Keywords: Optical fiber, co-packaged optics, 1310 nm, O-band, expanded-beam connector, high-power, external laser, reliability, contamination

1. INTRODUCTION

The advent of co-packaged optics (CPO) for data centers and high-performance computing, including machine learning and artificial intelligence (AI), represents a paradigm shift which introduces several new connectivity challenges. One such challenge for CPO architectures that incorporate off-chip, external laser (EL) sources [1] is to provide a reliable optical path for the laser power to the modulators on the chip. New ultra high-power continuous wave (CW) lasers demonstrated by Lumentum, operating at over 400 mW at 25 °C [2] enable a more efficient optical solution for the EL source in the CPO application. While the use of a high-power laser that is shared among many transmit (Tx) channels enhances reliability over the alternative of many low-power sources, system reliability can be further enhanced by use of EL pluggable modules that allow for replacement of a failed laser source with minimum disruption. This design requires the use of connectors between the pluggable laser source and the CPO harness connected to the switch substrate.

In some architectures, the ELs are coupled to the photonic integrated circuits (PICs) via multifiber connectors, with powers per wavelength in individual fiber channels reaching or exceeding 26 dBm [3]. Because the photonic integrated circuit (PIC) performance is sensitive to polarization state, it is usually assumed that polarization-maintaining fiber (PMF) will be used to deliver the light, with the birefringence axes precisely oriented at physical connections.

The use of very high power densities in these single-transverse-mode fibers combined with one or more connector interfaces evokes reliability concerns about failures triggered by contamination such as dust particles on the fiber end faces. In one study [4], clean single-mode physical-contact (PC) and angled-physical-contact (APC) connectors were found

to handle 1550 nm powers of 1 W or greater, but the damage threshold for some heavily contaminated connectors was <50 mW. That study also found that larger mode fields were correlated with higher damage thresholds.

Since the physical contact surfaces in CPO with EL sources cannot be guaranteed to remain free of contamination, the use of expanded beam (EB) connectors has been proposed [5] to mitigate the impact of contamination by taking advantage of the increase in damage threshold with mode field at a fixed contamination density as observed in previous studies [4]. Countering this advantage is the risk that particulates will slowly accumulate on the permanently exposed optical surfaces of the EB connectors and in some individual channels eventually bring the damage threshold below the service power levels.

There are other potential reliability issues. The connectors may slowly degrade under continuous exposure to these high powers and high power densities. Moreover, for multifiber connectors, if most or all of the channels are carrying high powers, the heat load from the connection losses may cause mechanical distortions that reduce the coupling efficiency. For example, a 12-fiber connector with an average of 0.1 dB (2.3%) loss for each channel and 250 mW in each fiber will dissipate about 70 mW (2.3% loss of a total 3 W transiting the connector).

We describe below some experiments to check the basic power-handling capability of an EB connector as well as its robustness against contamination.

2. HIGH-POWER TESTS OF AN EXPANDED BEAM CONNECTOR

We performed three experiments: a long-term single-channel high-power exposure test; a long-term "loop-back" test to pass power through multiple channels thus elevating the heating load on the connector; and a shorter-term contamination challenge to look for dust-induced failure.

2.1 Common Features

All experiments used the same Lumentum high-power O-band single-transverse-mode laser diode [6] and US Conec 16-channel MXC expanded beam connection (consisting of distinct "plug" and "receptable" connectors on ribbon jumpers with MTP connectors on the other ends). For convenience, PMF was not used for these tests, but rather Corning single-mode fiber. Since the mode field diameters at 1310 nm are similar for the two fiber types, the optical power densities and damage thresholds should also be very similar.

The laser was in a butterfly package with an internal thermo-electric cooler (TEC) and thermistor, seated in a Thorlabs laser mount and controlled through an NI™ LabVIEW interface. It was operated in constant current mode and with the temperature of the bottom of the laser submount kept at 25 °C by the internal TEC. Figure 1 below shows the LIV characteristics of the laser at 25 °C, which is capable of outputting 500 mW at a drive current of 1590 mA.

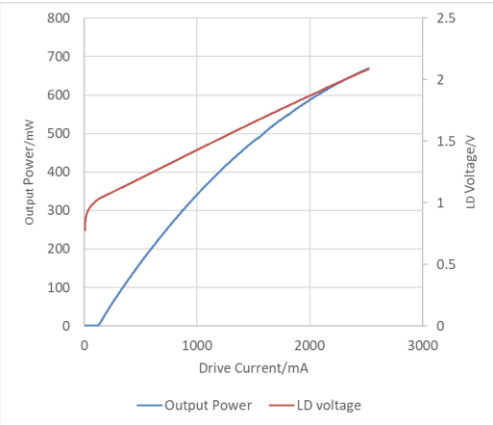

Figure 1: Laser ex-pigtail optical power and voltage vs drive current, with laser diode temperature at 25 °C, case temperature at 50 °C

The laser power was monitored with a photodiode (PD) on the 1% leg of a 99:1 tap placed after an isolator, and the optical power after passage through the sample under test was measured in a second meter at the output.

The laser wavelength was not measured or monitored, but according to the manufacturing data, at 25 °C submount temperature it was 1312-1313 nm over the operating drive current range.

The MXC connector pair assembled for this experiment used SM Prizm® MT prototype ferrules [7]. These assemblies, by intention, had moderately high losses on most channels ensuring that significant optical power was dissipated. Presumably, power dissipation occurred in the connector and perhaps the fiber segments immediately adjacent to the connector. Connection to the MXC® was made via input and output MTP® connectors. Before being incorporated into the experimental set-up, the MXC plug and receptacle lenses were inspected under a microscope.

The experimental optics and laser mount were inside an enclosure for safety, to avoid air currents and to buffer temperature changes in the laboratory ambient.

2.2 Single-Channel High-Power Exposure

For this experiment, the set-up was as shown in Figure 2 below. The output power was measured as the set-up was assembled to track the insertion loss (IL) of each stage. With the isolator, the IL between the FC/APC laser pigtail connector and the MXC input was 0.76 dB, and total initial loss from the laser pigtail connector to the output was 1.5 dB.

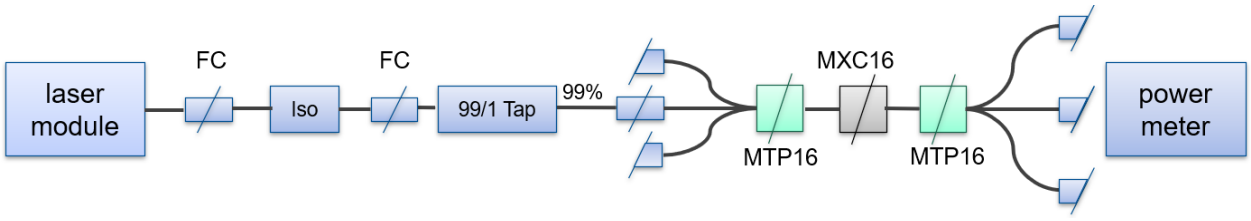

Figure 2: Set-up for Single-Channel Test. 16-channel MTPs are used to fan out the 16 channels of the 16-fiber MTP-MXC jumpers so that power can be coupled into the chosen channel. The unlabeled connectors are all single-fiber FC/APC format. The 1% tap leg leads to a power meter (not shown). For the first 644 hours of the test, the isolator was not present.

The laser current was set at 1240 mA, which delivered about 265 mW at the system output without the isolator; after the isolator was installed, the current was increased to 1370 mA giving 250 mW at the output.

2.3 "Loop-Back" High-Power Exposure

For the second experiment, the MXC channels were chained together so that the output power from one channel of the MXC was looped back as the input to its successor. The detailed layout is shown in Figure 3 below. This loop-back plan was designed to maximize the linear power loss in the middle channels of the MXC and to concentrate any heating near the middle channels.

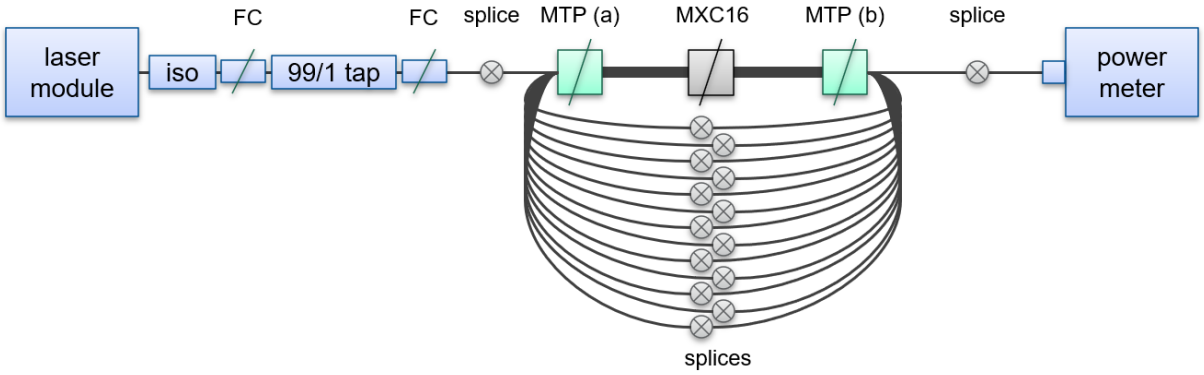

Figure 3: Configuration of Loop-Back Experiment.

Before the MTP-MXC jumpers were connected into the set-up, the recirculating loop-back link was spliced together. First, a ribbon MTP-MTP jumper was selected that had low loss on all channels for both ends, so that the average loss was 0.09 dB and the maximum loss was 0.27 dB. Two ribbon pigtails were made by cutting this jumper in half and the MTP ends were connected together. Each of the two resulting ribbon ends was split to extract individual fibers. First, the power out of the FC launch pigtail was measured, then light was launched into channel 8 of MTP (a) by splicing onto the pigtail. The power out of MTP (b) was then measured on the same channel. Then power was recirculated from the middle channels towards the outer channels while alternating splices on opposite sides of the connector. For example, channel 8 of MTP (b) was spliced to channel 9 of MTP (a), and then channel 9 of MTP (b) was spliced to channel 7 of MTP (a). Splicing ended with power out of channel 15 of MTP (b) so that channels 1 and 16 remained dark. After each splice, the power out of MTP (b) was measured to give the resulting accumulated loss in the recirculating link. Once the splice plan was complete, the MTP-to-MTP link was disconnected, the MTP-to-MXC and MXC-to-MTP jumpers were connected, and the power out of the entire link was measured. After splicing the MTP this way, the middle four channels accumulate about 67% of the power lost in the MXC, and the middle 6 about 79%.

Using the losses measured during assembly, the optical power lost at each connection interface and splice was computed for the estimated power of 432 mW input into MTP(a) channel 8. The estimated powers dissipated are given in Table 1., and the results are given in Figure 4 below, where the lost and incident powers at each successive connection along the light path are shown.

Table 1: Estimated optical power in mW lost at each connector, rows ordered by position of the channel in the loop-back path

Channel	MTP(a)	MXC	MTP(b)	Splice
08	30.7	45.7	25.3	1.5
09	31.0	31.0	25.2	1.1
07	38.6	21.3	29.0	0.7
10	4.1	13.0	3.6	0.6
06	4.4	13.1	3.8	0.5
11	2.5	8.4	2.2	0.4
05	5.3	10.1	4.4	0.3
12	5.9	5.5	5.0	0.3
04	3.2	6.1	2.7	0.2
13	3.7	3.8	3.1	0.2
03	2.9	3.4	2.4	0.1
14	1.2	2.0	1.0	0.1
02	1.8	2.0	1.5	0.1
15	1.1	1.4	1.0	0.1
TOTAL	**136.3**	**167.0**	**110.0**	**6.2**
TOTAL 07-10	**104.4**	**111.0**	**83.1**	**3.9**

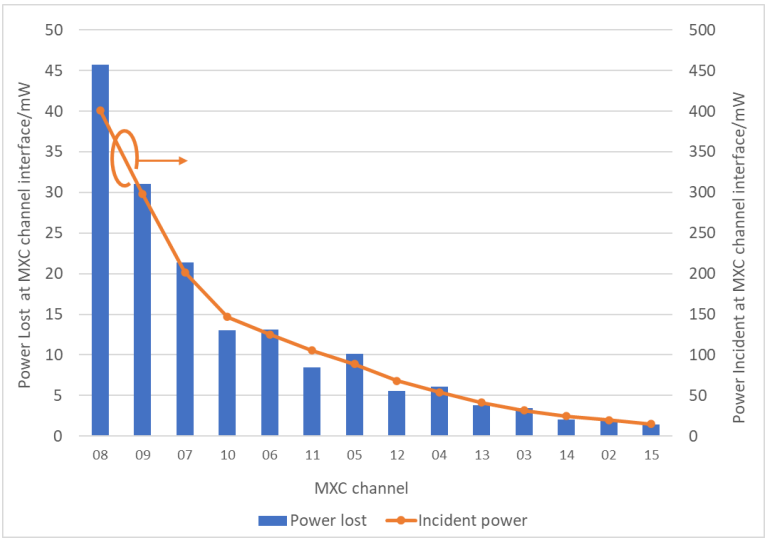

Figure 4: Estimated power loss and incident power at each MXC connection along the light path in the loop-back configuration, shown sequentially along the x-axis.

This experiment was performed after the single-channel test. The equipment was moved to a new laboratory and the isolator in the set-up was replaced with a high-power version. The laser drive current was raised to 1610 mA to achieve estimated 500 mW laser output power, or 432 mW at the input of the loop-back set-up. The laser power was stepped up to this setting over the course of a couple of days with intermediate power levels held for dwell times of about an hour, in order to identify the power threshold in the event of a catastrophic failure. No such failures occurred. The system was then left to run continuously at 1610 mA drive current. The experimental arrangement is shown in Figure 5.

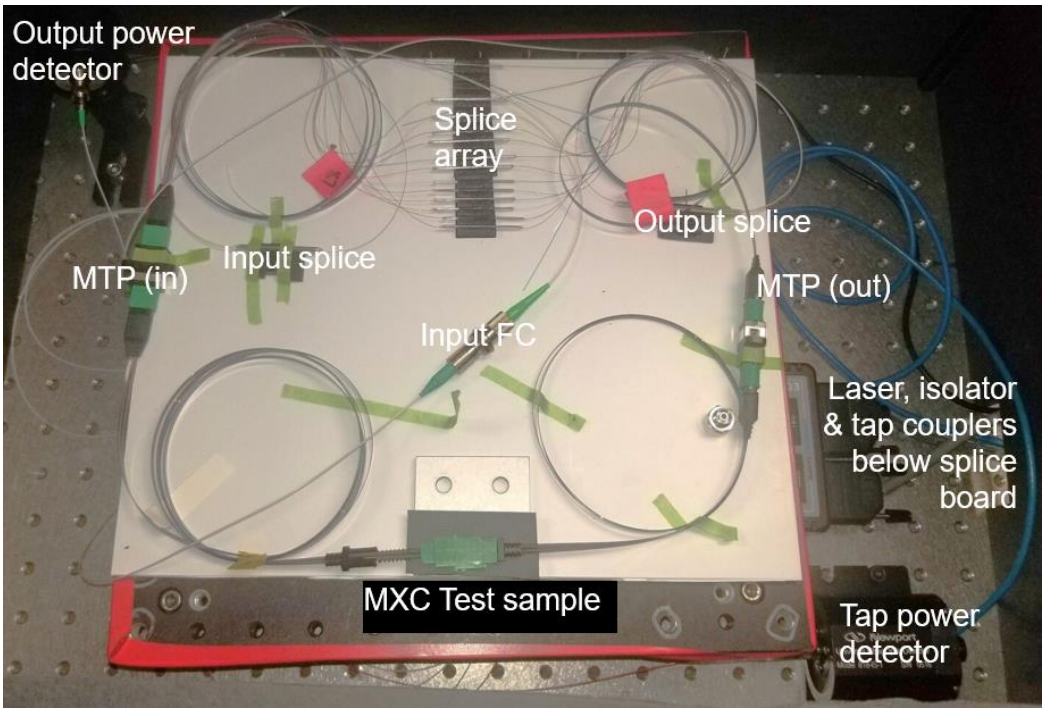

Figure 5: Loop-back Set-Up

We noticed some fluctuations with a range of a few percent in laser and output powers, and in the TEC current. Suspecting thermal effects, we installed three temperature sensors, one monitoring the lab temperature, one the air temperature in the laser enclosure and one the temperature of the MXC case. This last sensor in its supplied canister housing was initially just resting on the housing; later it was removed from its housing and the bare thermistor was held in place and in better thermal contact with the case by means of thermally conductive adhesive tape. The thermal data were logged to allow a comparison with the power and TEC current time series.

2.4 "Loop-Back" High-Power Exposure with Contamination Challenge

We wished to investigate the sensitivity of the MXC connector (Figure 6), which is not hermetically sealed, to particulates in the surrounding air, but without applying an unrealistic level of contamination. To this end, we moved the loop-back set-up to a significantly dirtier environment, as indicated by a count of airborne particle density, and introduced a vent and fan into the walls of the enclosure to ensure good circulation of the ambient air so that the air in the laser enclosure had the same contamination levels as that in the surrounding environment. We also placed the MXC on a TEC heater, and cycled the TEC temperature by ±10 °C around a central value of 25-30 °C. If the MXC cavity has half that temperature range, ±5 °C, on each 1-hour cycle 3% of the air in the MXC will be expelled and replaced as the air in the MXC interface cavity expands and contracts; over 20 hours 50% is replaced. This ensures that the particulate count inside the MXC volume quickly approaches that of the ambient air and tracks it with a half-life of less than a day.

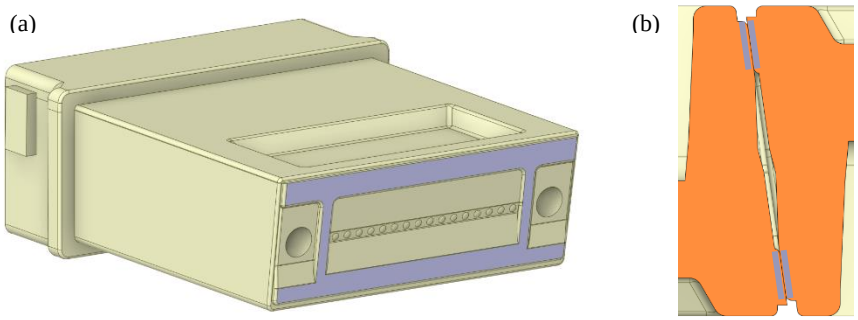

Figure 6: (a) MXC plug and (b) cross-sectional detail of mating region showing close contact around perimeter of cavity containing optical path.

The volume of the cavity is 0.37 mm^3; over a 10-year lifetime at one air exchange per day, 1.4 cm^3 of air would be passed through. The volume with appreciable optical power is much smaller, 0.003 mm^3.

2.5 Experimental Post-Mortem

At the end of the experiment, a multipath interference (MPI) measurement of the loop-back structure was made. The structure was then systematically dismantled to allow measurement of the IL of each interface. The MXC was disconnected and the lens faces inspected as far as possible.

3. EXPERIMENTAL RESULTS

3.1 Single-Channel High-Power Exposure

The single-channel condition with 265 mW out (before isolator installation, drive current 1.24 A) and 250 mW out (afterwards, 1.37 A) was run for a total of 2235 hours, continuously except for a few brief interruptions at the 644 hour mark for the isolator installation and modifications to the user interface software. We estimate that ~40 mW was being dissipated in the MXC connector in this condition.

The output power time series is shown in Figure 7 below. The laser and output powers were very stable over that entire period, with the output power varying by no more than ±1.8% before isolator installation and ±0.6% afterwards.

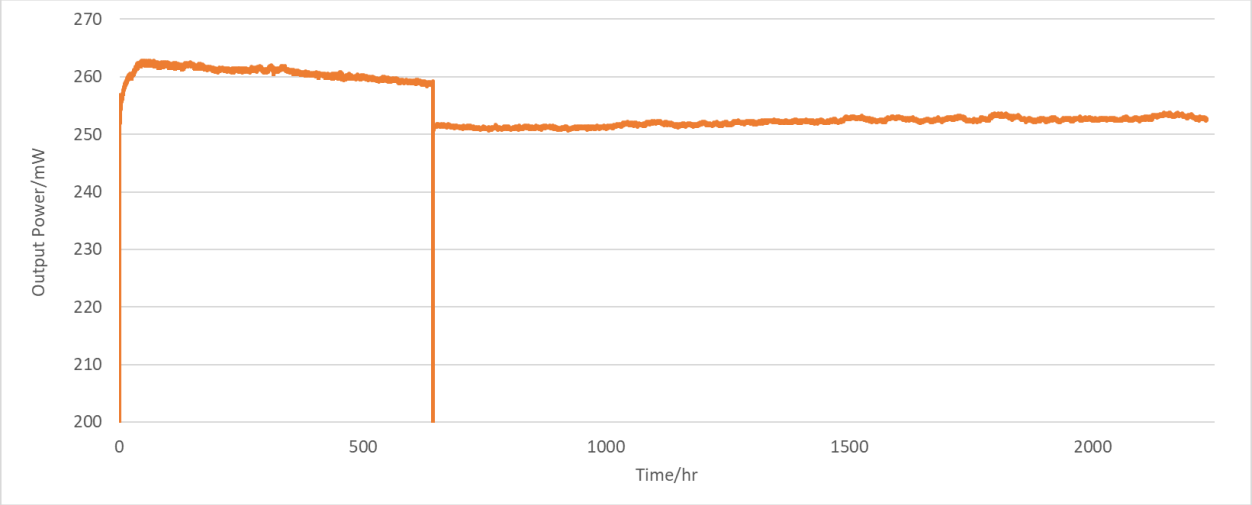

Figure 7: Power measured at output of MXC during the single-channel test. Variations in optical power are due to changes to the experimental configuration and thermal effects discussed in the text.

As the power was being stepped up in preparation for moving to the loop-back configuration, thermal transients were observed at higher powers as shown in Figure 8.

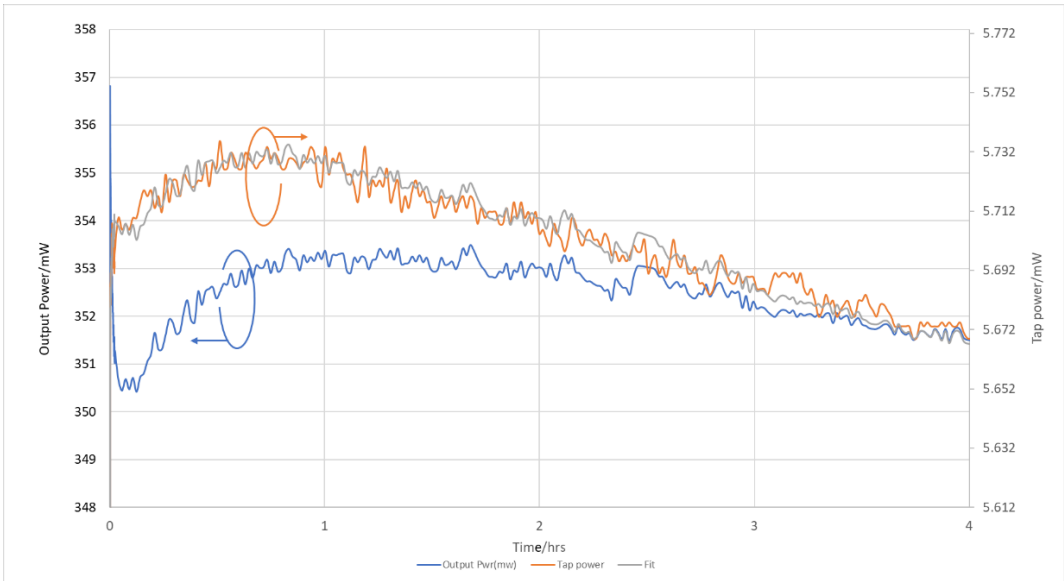

Figure 8: Start-up transients in the output power of the single-channel configuration. The gray line shows the output power corrected for the fitted double-exponential transients and scaled to match the tap power at later times.

The transient is reasonably well fitted by a sum of two exponential decays with very different time constants (31 s and 9760 s), with one component being a rapid but small (~2.5%) decline of the initial throughput power and the other a slow recovery of about half the power lost in the rapid decline. We speculate that the short time constant represents the effect of heating in the vicinity of the channel itself, and the longer time constant the effect of diffusion of heat from the laser mount through the experimental enclosure. The longer time constant is much longer than the expected thermal diffusion times for the ferrule alone. Note that we have not demonstrated that other channels show the same time-dependence in

their throughput power, and we didn't isolate the effect to the MXC – in particular, the MTPs might also show some time-dependent behavior as they heat up.

3.2 "Loop-Back" High-Power Exposure

The ramping of the single-channel power and then the loop-back configuration revealed no issues. The loop-back configuration then ran for 1460 hours with neither catastrophic failure nor slow degradation of the output power. As indicated in the previous section, through this period the MXC, MTP(a) and MTP(b) were respectively exposed to estimated dumped powers of 167 mW, 136 mW and 110 mW respectively, and total power fluxes (i.e. the sum of the input powers in all the channels) estimated at 1620 mW, 1760 mW and 1450 mW.

Fluctuations in laser and output powers and in the TEC current were observed during the loop-back test. After establishment of temperature monitoring, it was clear as shown in Figure 9 below that the laser and TEC variations were strongly correlated with the room temperature, which showed clear rapid upward excursions followed by slower declines that were mirrored in the laser and TEC data.

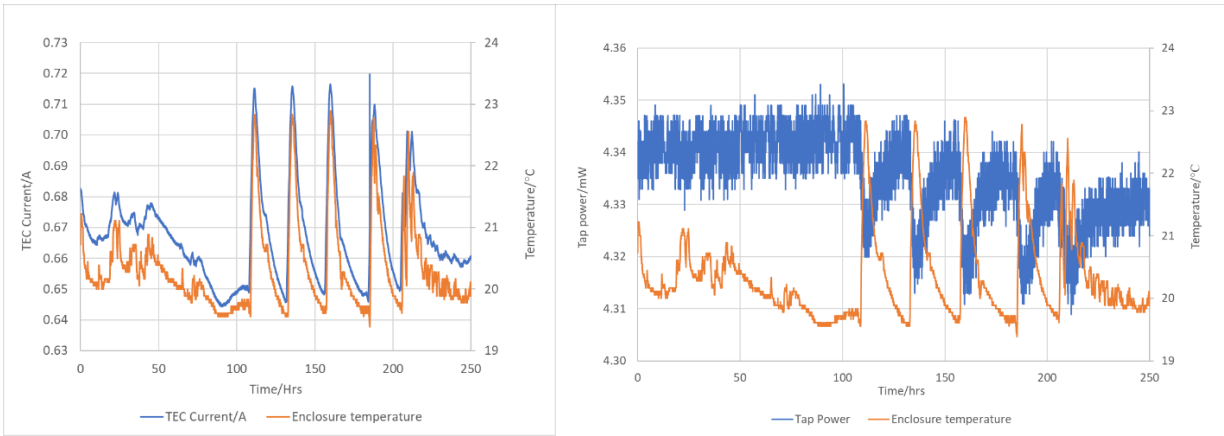

Figure 9: Fluctuations in TEC current and laser power are strongly correlated with laboratory temperature changes.

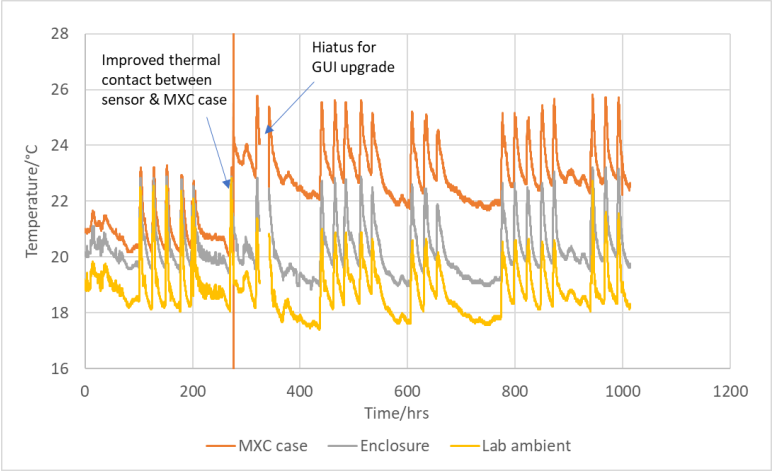

Figure 10: Temperature logs from three sensor locations

A comparison of the three temperature readings is given in Figure 10 above. The measured MXC case temperature increased noticeably when the thermal contact with the sensor was improved, running 3 °C higher than the enclosure temperature.

The full time series for the output power and laser tap power for the duration of the loop-back experiment are shown in Figure 11 below. The output power varies in a range of ±0.1 dB, while the tap power is significantly more stable, showing a decline of 1.6% (0.08 dB).

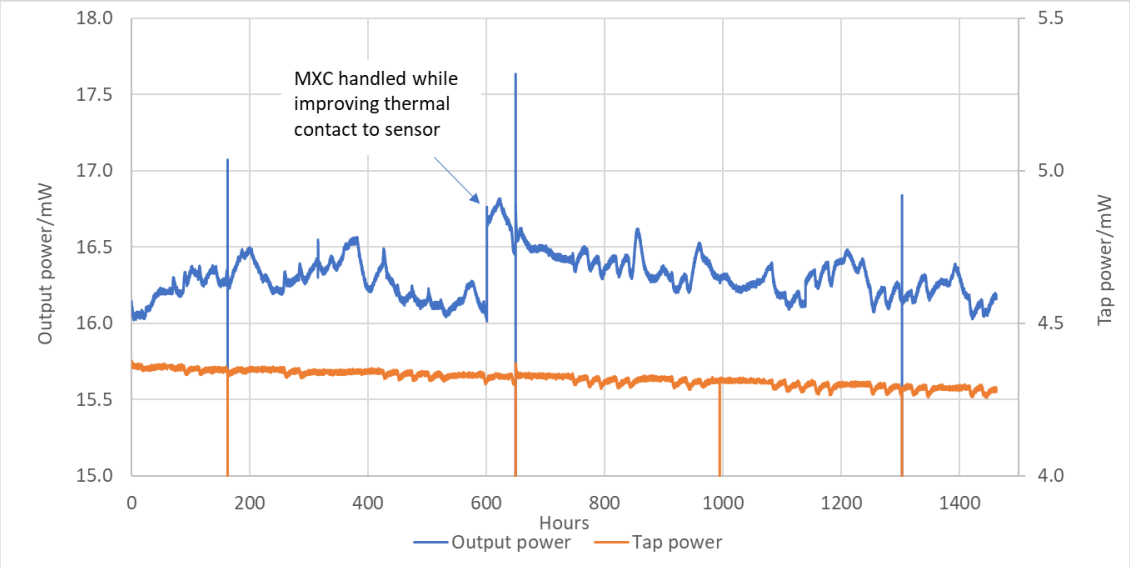

Figure 11: Time series of output power and tap power (scales with laser power) for loop-back configuration

As seen in Figure 12 the output power fluctuations showed some sensitivity to the MXC case temperature (after the thermal contact was improved the monitor readings were at least 3 °C higher than the ambient) but most of the ±2.4% variation followed a slow, meandering path quite inconsistent with the form of the temperature variations. We speculated that the bulk of the output power variation arises from MPI – the loop-back configuration is composed of 15 fairly short fiber segments between MTP and/or MXC connectors (even ignoring the splices), and the fibers are not tightly wrapped. Alternatively, or in addition, small uncorrelated changes in the IL at the multiple interfaces in the loop-back path could contribute – a uniform distribution of values within a range of 0.016 dB for each of the 42 MTP and MXC connections would produce the 0.03 dB standard deviation of the output power. If the variation is confined to the 14 MXC connections, the required range of variation would be 0.03 dB.

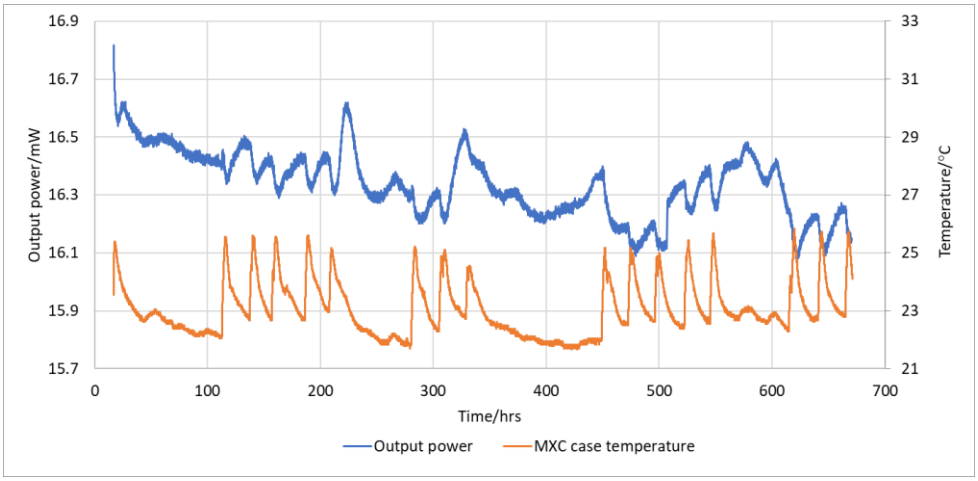

Figure 12: Time series for output power and MXC case temperature (period after contact of sensor to case was enhanced)

Although over the full loop-back experiment the output power did not show a tendency to decline, it had a bump up immediately after the MXC was handled to improve the thermal contact with the sensor, and then an apparent decline back to a level slightly higher than previously observed. As can be seen in Figure 13, the temperature difference between the MXC case and the interior of the laser enclosure showed a similar long-term drift, suggesting a thermomechanical cause for the power change.

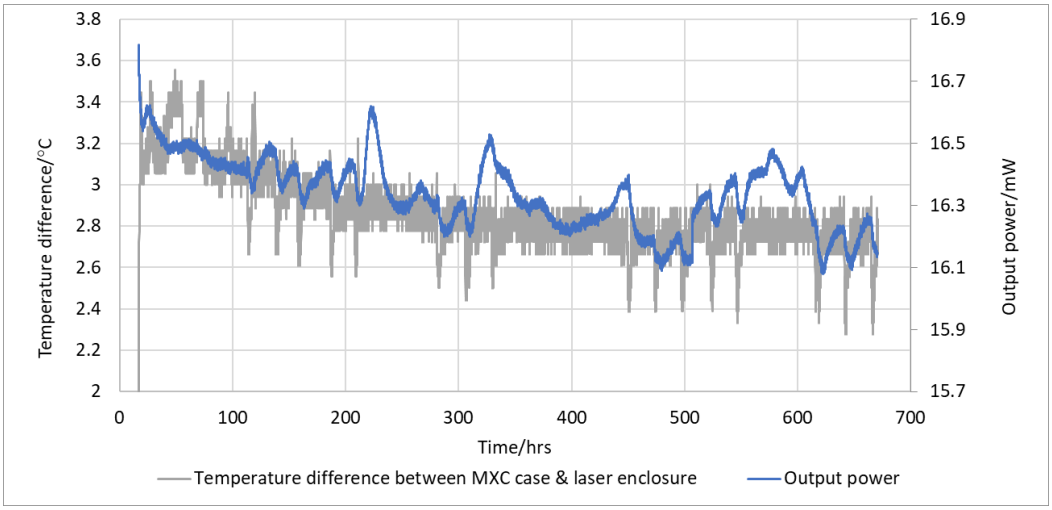

Figure 13: Showing qualitative similarity between declines in output power and in temperature difference between MXC case and laser enclosure

3.3 "Loop-Back" High-Power Contamination Challenge

The experimental enclosure was moved from the laboratory environment to a dustier location, as determined by counts of airborne particulates, see Table 2 below.

Table 2: Particulate Counts (particles/m^3) for lab and dusty location used for contamination challenge test

Particle size/µm	Lab Environment	Dusty Environment
0.3	3.12×10^5	1.64×10^6
0.5	1.74×10^4	2.05×10^5
5	2.47×10^2	1.64×10^4

The high-power test was restarted with the same laser current while ambient air was driven through the enclosure with a fan and a vent and the MXC case was heated on an hourly cycle with a 20 °C range as illustrated in Figure 14. This forced temperature cycle was more rapid and had a larger range than the laboratory temperature variation, where the laboratory had a periodic 24 hour temperature cycle with a range of about 8 °C and no air exchange was forced between the laboratory and the enclosure. The temperature was monitored on the top surface of the MXC, as before; the full range was ~3 °C, significantly lower than observed on the TEC.

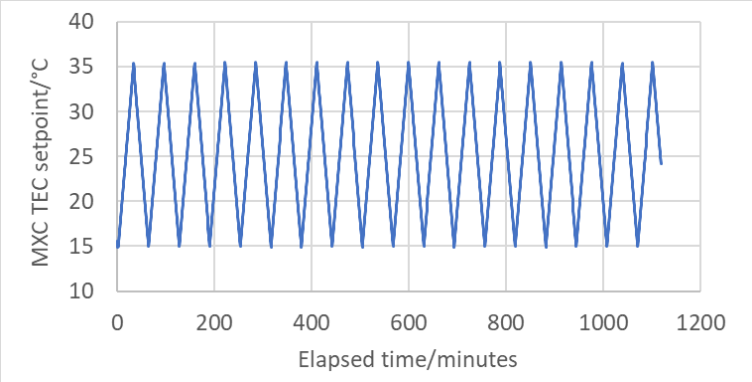

Figure 14: The thermal cycle initially applied to the TEC under the MXC case, with 20 °C full range and 1-hour period.

The results from the particle counter monitoring the air above the experimental enclosure are shown in Figure 15. The mean values were 22×10^{6}, 5.8×10^{3} and 8.7×10^{2} particles/m^3 for particle sizes >0.3 µm, >5.0 µm and >10.0 µm respectively, but there were large variations over the course of the experiment. For a total air volume of 1.4 cm^3 (1.4×10^{-6} m^3) passing through the MXC cavity over a 10-year lifetime, the expected number of entrained particles at these mean densities would be 31, 8×10^{-3} and 1×10^{-3} for sizes >0.3 µm, >5.0 µm and >10.0 µm respectively. Not all these particles would settle on the internal surfaces of the cavity, and fewer still on the lenses, of which the area with significant optical intensity is <1% of the cavity surface area (although the optical fields might affect the deposition rates). The average instantaneous number of particles in the three size ranges in the volume with optical power would be about 7×10^{-5}, 2×10^{-8} and 3×10^{-9} respectively. Thus we expected neither to see particles appear on the cavity surfaces after the contamination challenge test, nor to see short-term power variations from particles in the optical path. It should also be noted that while the connector is not hermetic there may be no path for larger particles to find their way into the cavity.

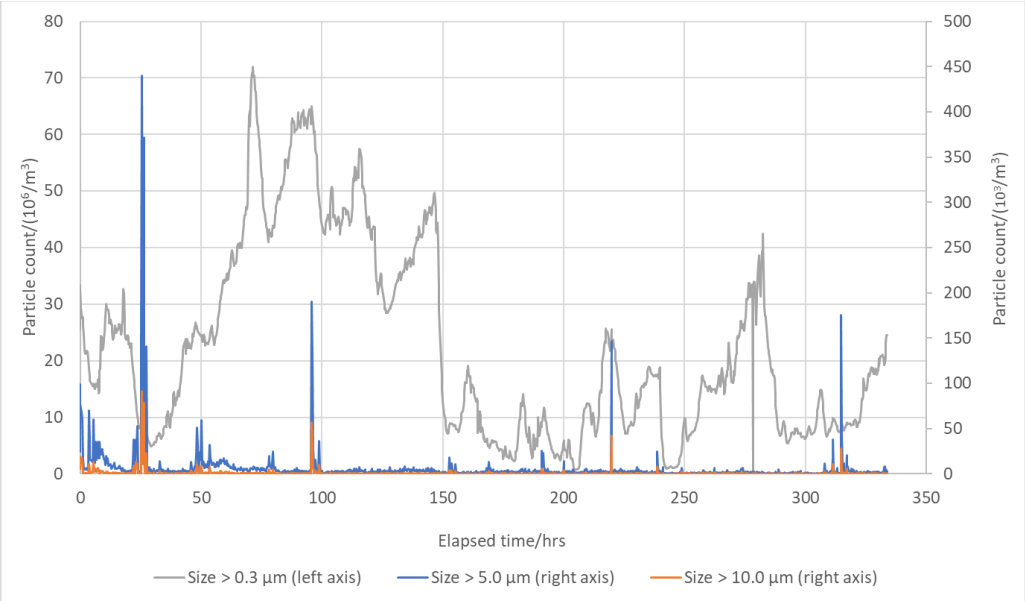

Figure 15: Output from particle counter for 3 different size ranges

Once again, the set-up ran for the entire test duration with neither catastrophic failure nor power degradation. The results are shown in Figure 16 below. The experiment was run during the long break in December 2023, and the TEC control was interrupted by errors over some of the run time (some of these control errors caused the laser to shut down), so the figure shows thick bands in the output power where the temperature was cycling, interspersed with periods of uncontrolled MXC temperature. The issue arose partly because the low set point of the temperature cycle was too cold and the TEC could not

always reach it. Ultimately we changed the cycle from 15-35 °C to 20-40 °C. The experiment lasted for 330 hours, but because of these issues the accumulated exposure time was 305 hours, and only 189 TEC cycles were completed.

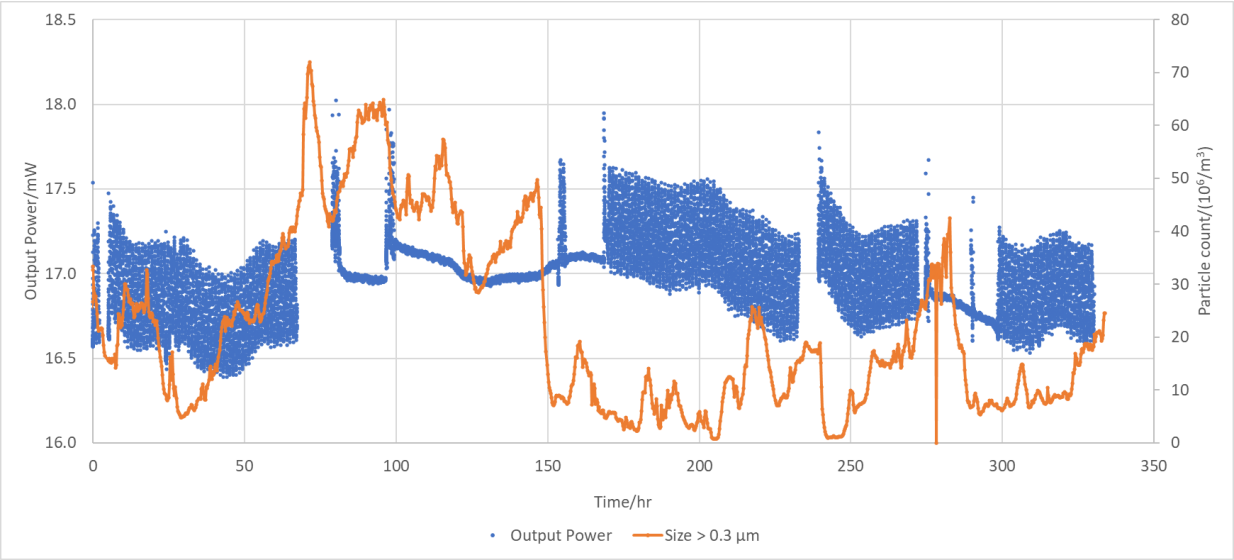

Figure 16: Output power from the loop-back configuration during the contamination challenge, and particle count monitored above the experimental enclosure. The thick bands correspond to power fluctuations driven by the temperature cycling.

As stated above, the TEC temperature range was 20 °C and the MXC top surface temperature range was 3 °C. We don't know the temperature range inside the MXC cavity, but the power range of 0.6 mW in the periods of thermal cycling is much larger than the roughly 0.1 mW fluctuations seen for ~3 °C temperature excursions shown in Figure 12 above. This suggests that the cavity temperature swings are also much larger, although the existence of a substantial temperature gradient across the MXC in this test means that the thermomechanical behavior may be different and previous findings are not directly applicable. If we assume that the air temperature in the MXC cavity varies over a range of 10 °C, half the TEC temperature range, then each cycle should exchange ~3.3% of the air, with a "half-life" of 20 cycles. i.e. 20 hours.

When the test was completed, an MPI measurement [8] was made (without high-loss offset input and output splices) on the loop-back configuration, with the results in Figure 17. The loop-back system has high and unstable MPI, with power variations of 0.2 to 0.3 dB at 1310 nm, large enough to account for the output power fluctuations in the high-power test.

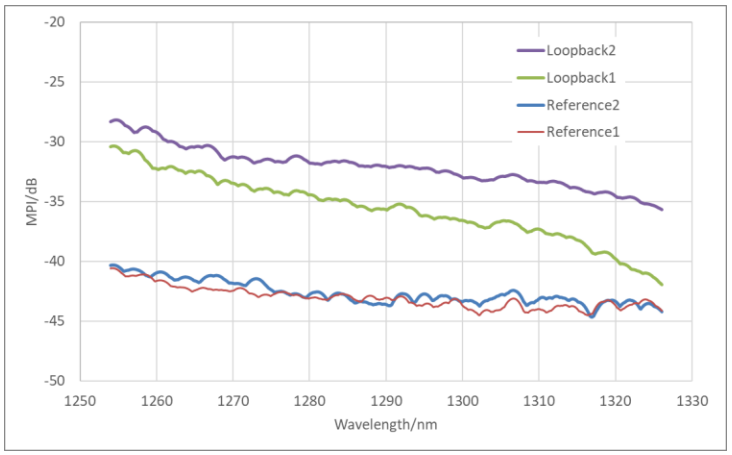

Figure 17: MPI for loop-back structure compared to a reference (1 m Corning SMF-28® Ultra fiber laid out straight). The reference measurement is made without the loop-back structure in the measured link.

The structure was then systematically disassembled with IL measurements for each stage of disassembly. Finally, the lens surfaces of the male part of the MXC connector pair were examined for damage and contamination, with resolution on the order of 1 μm. No damage was observed, and no newly arrived particulates were noted on the lenses, although the resolution of the "before" images restricts this observation to particles with dimensions over about 10 μm.

4. SUMMARY

We studied the behavior of a single-mode MXC expanded-beam connector when exposed to high power in the O-band and associated elevated temperature in the connector. We ran tests in two regimes – a single-channel exposure of approximately 310 mW input power and a multichannel, "loop-back" exposure that dumped an estimated 167 mW in the connector and its vicinity with individual channels in the MXC connector exposed to as much as 400 mW of optical power. The single-channel exposure ran for ~2235 hours, and the "loop-back" exposure for 1460 hours in a relatively clean laboratory followed by another 305 hours in a dirty environment, with the air in the MXC cavity forced to exchange with the ambient by seating it on a TEC with its temperature cycling over a range of 20 ºC every hour.

We observed neither catastrophic failures nor slow power degradation, with the MXC and the MTPs supporting the high optical powers. We did see small start-up transients, and in the single-channel case, the transient seemed to have two very different time constants, an immediate decrease in output power of 2.5% with a 1/e time of 31 s and a slower recovery of about half the initial drop with a 1/e time of 9760 s. We speculate that the short time constant may be associated with local heating of the channel carrying the laser power, and the longer time constant with diffusion of heat through the experimental enclosure from the laser mount. We also saw slow drifts in output power, which were more marked for the loop-back test, but these seem to have arisen from multipath interference and thermal effects, with no evidence for degradation of the connector. After the exposure to a dusty environment, the lens surfaces of the MXC showed no particulate contamination that had not been present at the beginning of the first experiment.

REFERENCES

[1] Tan, M., Xu, J., Liu, S., Feng, J., Zhang, H., Yao, C., Chen, S., Guo, H., Han, G., Wen, Z., Chen, B., He, Y., Zheng, X., Ming, D., Tu, Y., Fu, Q., Qi, N., Li, D., Geng, L., Wen, S., Yang, F., He, H., Liu, F., Xue, H., Wang, Y., Qiu, C., Mi, G., Li, Y., Chang, T., Lai, M., Zhang, L., Hao, Q. and Qin, M., "Co-packaged optics (CPO): status, challenges and solutions," *Frontiers of Optoelectronics*, vol. 16, no. 1 (2023).

[2] Lumentum Inc., https://investor.lumentum.com/financial-news-releases/news-details/2023/Lumentum-Addresses-Surge-in-AI-and-ML-Data-Traffic-with-High-Performance-Optical-Solutions-at-ECOC-2023/default.aspx.

[3] Optical Internetworking Forum, "Implementation Agreement for a 3.2Tb/s Co-Packaged (CPO) Module," Optical Internetworking Forum, Fremont, CA, USA (2023).

[4] De Rosa, M., Carberry, J., Bhagavatula, V., Wagner, K. and Saravanos, C., "High-Power Performance of Single-Mode Fiber-Optic Connectors," *Journal of Lightwave Technology*, vol. 20, pp. 851-857 (2002).

[5] T. Mitcheltree, "CPO Optical Connectivity Considerations," 4 May 2022. [Online]. Available: https://www.onboardoptics.org/_files/ugd/8abe6c_ec32273fed814e80bbd93bd66364a7fa.pdf. [Accessed 8 January 2024].

[6] Zhou, W., Zhu, Y., Wang, J., Moewe, M., Zhu, R., Zhao, W., Rossin, V., Liu, H., Wang, J., Zhu, T., Yalamanchili, P., Pham, T., Chen, R., Zeng, V. and Stewart, J., "High Power CW Laser for Co-Packaged Optics," *Conference on Lasers and Electro-Optics*, paper SS2D.3 (2022).

[7] Kadar-Kallen, M., Kurtz, D., Lutz, S., Schoellner, D., Wang, K., Fortusini, D., and Modavis, R., "Single-Mode Expanded Beam MT Connector with Angled Lens Array for Improved Optical Performance," *2022 European Conference on Optical Communication*, paper Tu5.4 (2022).

[8] Recommendation ITU-T G.650.1 (2018), "Definitions and test methods for linear, deterministic attributes of single-mode fibre and cable" International Telecommunication Union (2018)